ACS APPLIED MATERIALS & INTERFACES

Research Article

www.acsami.org

Fully Solution-Processing Route toward Highly Transparent Polymer Solar Cells

Fei Guo,*[,†] Peter Kubis,[†,‡] Tobias Stubhan,[†] Ning Li,[†] Derya Baran,[†] Thomas Przybilla,[§] Erdmann Spiecker,[§] Karen Forberich,[†] and Christoph J. Brabec*[,†,#]

[†]Institute of Materials for Electronics and Energy Technology (i-MEET), Friedrich-Alexander-University Erlangen-Nuremberg, Martensstrasse 7, 91058 Erlangen, Germany

[‡]Erlangen Graduate School in Advanced Optical Technologies (SAOT), Friedrich-Alexander-University Erlangen-Nuremberg, Paul-Gordan-Strasse 6, 91052 Erlangen, Germany

[§]Center for Nanoanalysis and Electron Microscopy (CENEM), University Erlangen-Nuremberg, Cauerstraße 6, 91058 Erlangen, Germany

[#]Bavarian Center for Applied Energy Research (ZAE Bayern), Haberstrasse 2a, 91058 Erlangen, Germany

Supporting Information

ABSTRACT: We report highly transparent polymer solar cells using metallic silver nanowires (AgNWs) as both the electron- and hole-collecting electrodes. The entire stack of the devices is processed from solution using a doctor blading technique. A thin layer of zinc oxide nanoparticles is introduced between photoactive layer and top AgNW electrode which plays decisive roles in device functionality: it serves as a mechanical foundation which allows the solution-deposition of top AgNWs, and more importantly it facilitates charge carriers extraction due to the better energy level alignment and the formation of ohmic contacts between the active layer/ZnO and ZnO/AgNWs. The resulting semitransparent polymer:fullerene solar cells showed a power conversion efficiency of 2.9%, which is 72% of the efficiency of an opaque reference device. Moreover, an average transmittance of 41% in the wavelength range of 400−800 nm is achieved, which is of particular interest for applications in transparent architectures.

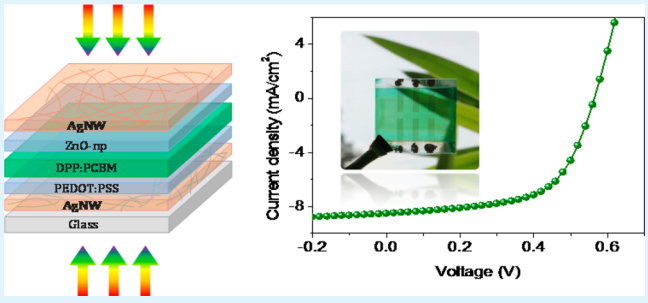

KEYWORDS: *semitransparent polymer solar cells, fully solution-processing, OPV, ITO-free*

1. INTRODUCTION

Bulk-heterojunction polymer solar cells (PSCs) have been recognized as an attractive solar technology because of the promise of low-cost materials and easy processing requirements.[1,2] The intrinsic features of color tunability and semitransparency of the thin photoactive films turn out to be a great asset for PSCs. These characteristics enable the manufacturing of differently colored semitransparent PSCs (ST-PSCs) by applying two transparent electrodes.[3−12] In addition to traditional applications similar to inorganic panels, aesthetic ST-PSCs are quite appealing power generators for various transparent architectures, such as windows, glass roof tops, curtain walls, shades, self-powered greenhouses, etc. Because of these specific applications, ST-PSCs have recently attracted growing attention and are considered as a high priority for organic photovoltaics (OPV).

By employing high-performance photoactive polymers,[4−6] tandem structures,[7−9] and advanced light management,[10−12] the power conversion efficiency (PCE) of ST-PSCs was steadily increased to over 7%. Despite this progress in pursuing high efficiencies, only a few reports have focused on the low-cost solution-processing of the entire device stack. Many reported ST-PSCs currently employ commercial indium tin oxide (ITO) as bottom electrodes combined with a vacuum deposited or sputtered transparent top electrodes, i.e., ITO or thin metal films.[4−18] However, the utilization of expensive ITO (caused by the scarce indium and the involved sputter and tempering procedures) and energy-consuming deposition of top electrodes are unfavorable to fulfill the cost potential of the PSC technology. Accordingly, it is highly desired that a cost-effective fully solution-processing route that is compatible with roll-to-roll manufacturing can be developed to fabricate semitransparent solar cells.

To realize fully solution-processed ST-PSCs, the selection of electrode materials and corresponding processing technique are the two important considerations. Several solution-processable electrodes,[19,20] such as carbon nanotubes, graphene, printed silver grids, highly conductive poly(3,4-ethylenedioxythiophene):poly(styrenesulfonate) (PEDOT:PSS), metallic nanowires/nanoparticles, etc., have been

Received: August 11, 2014
Accepted: September 19, 2014
Published: September 19, 2014

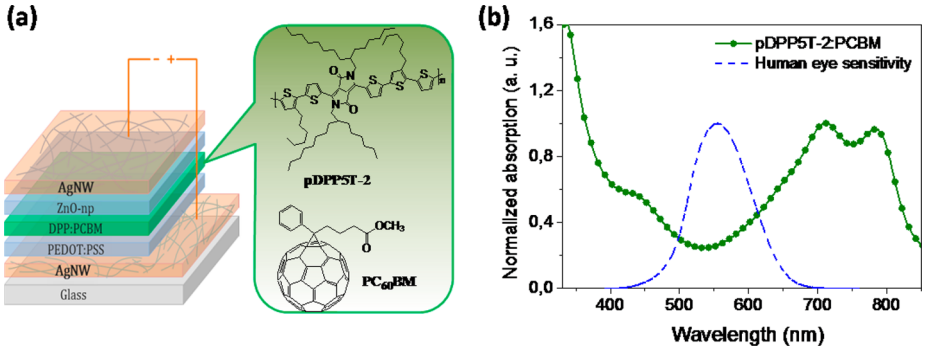

Figure 1. (a) Schematic architecture of the entire solution-processed semitransparent solar cell AgNW-AgNW and chemical structures of the donor pDPP5T-2 and acceptor $PC_{60}BM$. (b) Normalized absorption spectrum of the photoactive layer film and the curve of human eye sensitivity.

proposed as alternative bottom electrodes to ITO for organic optoelectronic devices. Among these materials, silver nanowires (AgNWs), because of their outstanding optical and electrical properties and solution processability, have been demonstrated as the most promising candidate.[21−24] However, because the active layer thickness of PSCs is typically lower than 200 nm, a major difficulty for achieving fully solution-processed ST-PSCs remains the integration of solution-processed top electrodes without compromising the device performance. Spray coating has recently been adopted by several groups to deposit top electrodes for PSCs and solid-state dye-sensitized solar cells without significantly deteriorating the device performance.[4,6,8,15,23,26] Despite these achievements, it is generally observed that fully solution-processed PSC devices showed a rather inferior performance compared to their evaporated counterparts.

Previously, we have demonstrated fully solution-processed ST-PSCs with a 33% visible transparency.[27] In those inverted devices, however, the hole-transport layer PEDOT:PSS was too thin and too soft to withstand doctor-blading of AgNWs from water-based solution. As a result, we had to shift to spray coating for the deposition of the top AgNWs electrode, which increased the complexity in device fabrication. Successively, Yim also reported fully solution-processed semitransparent PSCs in an inverted structure employing AgNWs and PEDOT:PSS as bottom and top electrodes, respectively.[28] However, the involved wide bandgap absorber poly(3-hexylthiophene-2,5-diyl) and relatively low conductive PEDOT:PSS top electrode adversely resulted in the devices with low FFs and low visible transparency.

It should be noted that to fabricate semitransparent solar cells, the trade-off between the efficiency and transparency of the devices should always be considered. Ideally, solar cells with high efficiency while maintaining high transparency are highly desirable. This requires that light absorber material features the minimal absorption in the visible range. In this work, through a rational interface engineering combined with a judicious choice of photoactive material we report facile fabrication of highly transparent PSCs in a normal device structure. The entire device stack was solution-processed by a roll-to-roll compatible doctor blading technique under ambient conditions. AgNW meshes were used as both the anode and cathode contacts. One major challenge for the realization of the fully solution-processed normal structure ST-PSCs is the substitution of the evaporated low work function LiF/Al or Ca/Ag electrodes by their printable analogs. As the most decisive step, we introduced a thin layer of zinc oxide nanoparticles (ZnO) between the photoactive layer and top AgNW electrode. Because of the excellent compatibility of the two buffer layers, PEDOT:PSS and ZnO, with the solution processing of AgNWs, the as-prepared semitransparent devices showed high FFs of 61% with PCEs of 2.9%.

2. RESULTS AND DISCUSSION

Figure 1a shows the schematic architecture of the fully solution-processed ST-PSCs in a normal structure with a layer sequence of glass/AgNW/PEDOT:PSS/photoactive layer/ZnO/AgNW. We designate this fully solution-processed solar cell as AgNW-AgNW. To obtain a comprehensive evaluation of the fully solution-processed devices, we simultaneously fabricated another three reference cells with different electrode configurations, named as ITO-Ag, ITO-AgNW and AgNW-Ag, in which the photoactive layer and the two interface layers remain unchanged. A bulk heterojunction blend consisting of a low bandgap polymer based on diketopyrrolopyrrole (pDPP5T-2) as donor and [6,6]-phenyl-C_{60}-butyric acid methyl ester ($PC_{60}BM$) as acceptor (1:2 wt %) was employed as photoactive layer. Chemical structures of the two materials and the absorption spectrum of the photoactive blend film are shown in Figure 1a and Figure 1b, respectively. It can be seen that the absorption spectrum of the photoactive layer extends to the near-infrared region until ∼900 nm, with the strongest absorption range located between 600 and 850 nm and the lowest absorption around 550 nm where the human eye is most sensitive. A blend of pDPP5T-2 with $PC_{60}BM$ is therefore ideally suited for semitransparent solar cells from an optical point of view.

We note that opaque devices with the active layer consisting of pDPP5T-2 and $PC_{70}BM$ can provide efficiencies of close to 6%.[29] Here, we choose $PC_{60}BM$ because of its negligible absorption in the visible regime, which allows us to fabricate semitransparent devices with high visible transparency without sacrificing absorber layer thickness.

SEM images of our AgNWs shown in Figure S1 in the Supporting Information indicate that the diameter and length of the nanowire is around 30 nm and 10−30 um, respectively, whereas the voids within the NW network are below 500 nm. Although AgNWs are a percolation network type electrode, it is widely observed that the voids between the NW network do not negatively affect the charge carriers collection.[21−24] Another critical concern associated with AgNW electrodes is their high surface roughness which is generally in the range of tens of nanometers. Therefore, to prevent possible short-circuit of the devices, surface modifications are generally required to

smoothen out the surface of AgNWs.[21−24,30] Herein, a 40 nm thick PEDOT:PSS was coated to fill the AgNW network and functioned as a hole transport layer to enhance the charge carrier selectivity. Images a and b in Figure 2 show atomic force

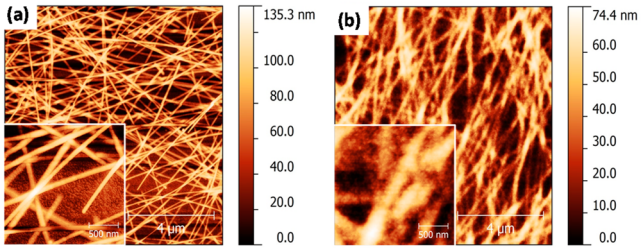

Figure 2. (a) AFM images (10 × 10 μm) of as-bladed bottom AgNW electrode; (b) AgNW networks coated with a layer of PEDOT:PSS. The insets of a and b show the corresponding small area (2 × 2 μm) AFM images.

microscope images of the doctor bladed AgNW film on glass and the film coated with a layer of PEDOT:PSS, respectively. It was observed that the unmodified AgNW film showed a root-mean-square roughness of ∼13 nm which was reduced to ∼7 nm by covering a layer of PEDOT:PSS. Comparing the insets of Figure 2a, b, one can clearly see that the polymer PEDOT:PSS not only wrapped the individual AgNWs but also filled the empty space between the NWs, resulting in a rolling-hill morphology.

For traditional opaque PSCs with a normal structure, it is straightforward to thermally evaporate a thin layer of LiF/Al or Ca/Ag as top electrodes. In our fully solution-processed devices, we found that the deposition of AgNWs from water-based solution onto the active layer has a pronounced wetting problem due to the low surface energy of the organic film. In addition, the energy level mismatch between the photoactive polymer and the AgNW electrode indeed requires an electron transport layer to facilitate electron extraction. Therefore, prior to the deposition of the AgNW top electrodes, we bladed a ∼50 nm-thick ZnO nanoparticle layer from isopropanol based solution on top of the active layer. Compared to the device without ZnO modification, the applied ZnO layer allows for uniform deposition of AgNWs film without any wetting problem (see Figure S2 in the Supporting Information). More importantly, we note that the introduction of the ZnO layer plays an essential role in the device functionality: because of a better energy level alignment and the formation of an ohmic contact between the ZnO and AgNWs (see Figure S3 in the Supporting Information), the ZnO layer can effectively eliminate the energy barrier for electron extraction.

On the basis of the device architecture discussed above, we produced the fully solution-processed semitransparent device AgNW-AgNW. The device fabrication procedure is schematically illustrated in Figure 3. The entire processing of the devices including the deposition of two electrodes, interface layers and photoactive layer was carried out by doctor blading in ambient atmosphere. The detailed device fabrication procedure is presented in the Experimental Section. As a first step, we bladed AgNWs on glass substrate and subsequently patterned the as-coated NW film by laser sintering to obtain six electrodes.[31] It is known that laser structuring usually requires additional cleaning steps to remove the debris resulting from the ablation process. To prevent short-circuiting of the devices, the as-patterned AgNW electrodes were dipped in water to wash away the debris particles remaining on the patterned areas. Optical microscopy images shown in Figure S4 in the Supporting Information evidenced a thorough removal of the remaining particles by dipping in water for 30 s.

Figure 4 shows a cross-sectional scanning electron microscopy (SEM) image of a completed AgNW-AgNW

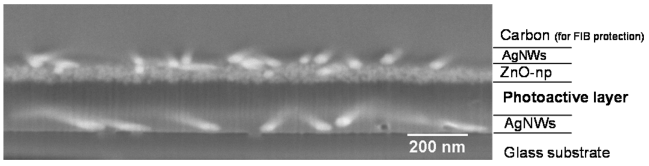

Figure 4. Cross-sectional SEM image (tilted view) reveals the layer sequence and structure. Note that the PEDOT:PSS layer cannot be distinguished from the photoactive layer in the SEM image.

solar cell. From the SEM image, we can see that both the bottom and top AgNW electrodes can be clearly distinguished. Remarkably, distinct interfaces between the photoactive layer/ZnO and ZnO/AgNWs without interlayers mixing are resolved. It is worth mentioning that these observations anticipate full device performance without detrimental effects from shunting or surface recombination.

Figure 5a shows the current density−voltage (J−V) charateristics of the fully solution-processed semitransparent device AgNW-AgNW and the three control devices, which were measured under one sun with simulated AM 1.5G irradiation at 100 mW cm^{-2}. The two semitransparent devices ITO-AgNW

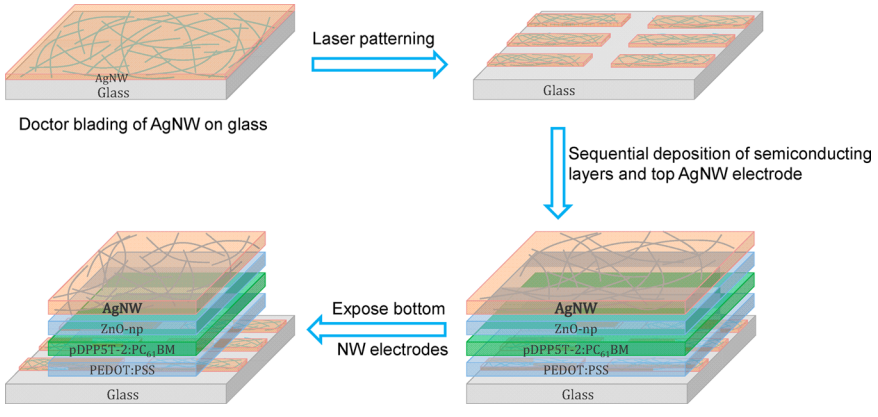

Figure 3. Schematic illustration of the fully solution processing of the ST-PSCs using AgNWs as both the bottom and top transparent electrodes.

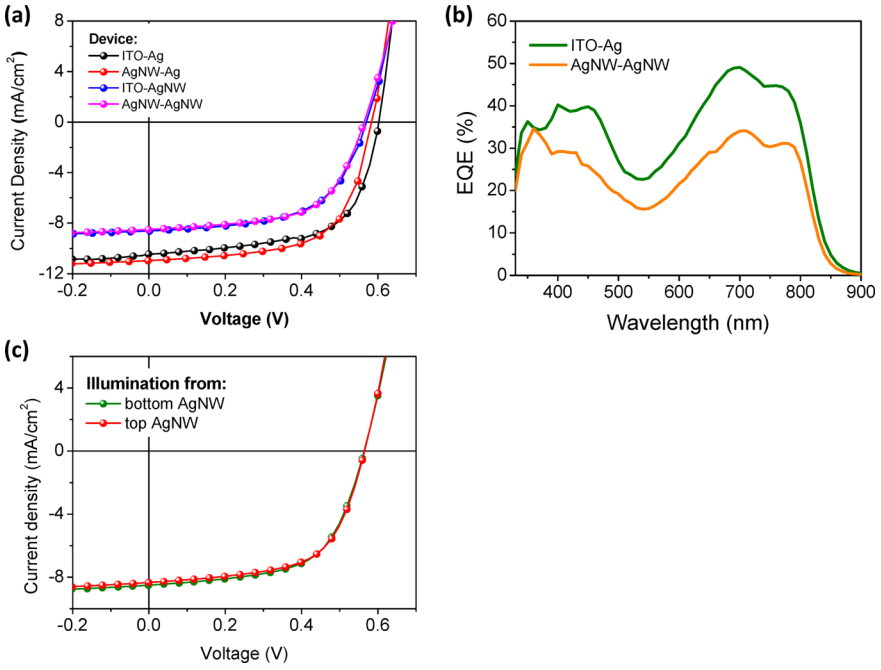

Figure 5. (a) J–V curves of the four investigated devices. (b) The EQE characteristics of the fully solution-processed device AgNW-AgNW and the reference ITO-Ag. (c) J-V curves of the device AgNW-AgNW under different illumination directions.

Table 1. Summary of the Performance of the Investigated Devices

device	V_{oc} (mV)	J_{sc} (mA/cm^2)	FF (%)	PCE (%)	R_p (kΩ cm^2)	R_s (Ω cm^2)
ITO-Ag	602	10.45 (10.80)*	62.88	3.96	44.50	0.94
AgNW-Ag	583	10.96	63.11	4.03	12.27	1.27
ITO-AgNW	570	8.62	57.86	2.84	397.51	3.49
AgNW-AgNW (bottom illumination)	559	8.24 (8.05)*	60.94	2.87	18.37	4.92
AgNW-AgNW (Top illumination)	559	8.48	60.22	2.89		

Note: *the J_{sc} values are calculated by convoluting the EQE curves with the standard AM 1.5G solar spectrum. The difference between the calculated J_{sc} and measured J_{sc} values are within 5%, indicating a good accuracy of our PSCs measurement.

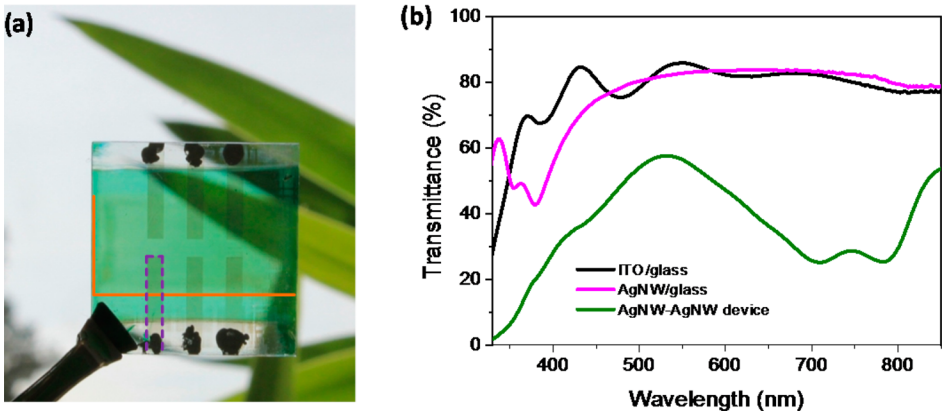

Figure 6. (a) A digital photograph of the as-fabricated semitransparent AgNW-AgNW device. The rectangular areas of the orange solid line and purple dashed line respectively indicate top and bottom AgNW electrode. The active area is defined by the overlapping region of the two electrodes. Silver paste was applied to increase the contact between AgNW electrodes and the measurement probes. (b) Transmittance spectra of AgNW-coated glass and commercial ITO-coated glass and the semitransparent device AgNW-AgNW.

and AgNW-AgNW were encapsulated in a N_2-filled glovebox before testing the photoelectric behaviors in ambient air. As shown in Figure 5a, the two opaque reference devices with a reflective Ag top electrode, ITO-Ag, and AgNW-Ag, showed similar performances with $J_{sc} \approx 11.0$ mA/cm^2, $V_{oc} = 0.58$–0.60 V, and FF of ∼63%, yielding a PCE of ∼4.0%. These results suggest that AgNWs are an ideal alternative to ITO as window electrode for PSCs owing to their comparable optoelectronic properties, and that the higher surfance roughness of the NW network did not negatively affect the device performance. Due to the lack of reflective back electrodes, the two semi-transparent devices showed J_{sc} of approximately 8 mA/cm^2,

which is about 3 mA/cm^2 lower than for the opaque counterparts. It should also be noted that the devices with top solution-processed AgNW electrodes showed a slightly lower FF (61% as compared to 63%) than the evaporated devices, which is consistent with previous studies.[4,14,15,27,28,32,33] We attribute this performance decrease to the higher contact resistance of the solution-processed electrodes with the underlying interfacial layers, which impairs charge extraction. Indeed, in our solution-processed semitransparent devices, the series resistance derived from the $J-V$ curves measured in the dark (see Figure S5 in the Supporting Information) is 3−5 times higher than for the opaque devices with evaporated Ag electrodes (Table 1).

External quantum efficiency (EQE) characterizations of the reference device ITO-Ag and fully solution-processed AgNW-AgNW cell were performed to investigate their photoresponse behaviors. As depicted in Figure 5b, both devices exhibit two EQE peaks in the range of 350−450 nm and 650−800 nm, with a low photoresponse around 550 nm, corresponding to the high transmittance measured at this wavelength. The semitransparent device AgNW-AgNW showed lower EQE values in the entire wavelegth range mainly because of the transmittance losses. We have also compared the performance of AgNW-AgNW device with illumination from either the bottom or the top electrode. As shown in Figure 5c, the AgNW-AgNW device exhibited an identical performance in terms of V_{oc}, J_{sc}, FF, and PCE independent of illumination direction, suggesting comparable optoelectronic performance of both the bottom and top AgNW electrodes. Indeed, independent measurements of the bottom AgNW coated on glass and the top AgNW coated on ZnO film showed a similar optoelectronic properties, as indicated in Figure S6 in the Supporting Information. The key device performance parameters are summarized in Table 1.

R_p and R_s represent parallel resistance and series resistance, which are calculated from the slope of the dark $J-V$ curves at −1 and 2 V bias, respectively.

Figure 6a shows a digital image of the as-fabricated highly semitransparent AgNW-AgNW device through which the leaves behind can be clearly seen. The transmittance spectra of the AgNW-AgNW device as well as the ITO and AgNW electrodes employed in the present work are displayed in Figure 6b. It can be seen that the AgNW electrode ($R_{\square}$ = 9 Ω sq^{-1} and T = 88% at 550 nm) shows a comparably high but more flat transmittance characteristics than the ITO in the visible region of 450−850 nm. This feature makes AgNWs an ideal electrode material for optoelectronic applications, i.e., PVs and light emitting diodes, etc. Our fully solution-processed AgNW-AgNW solar cell shows transmittance of 56% at 550 nm wavelength where the human eye is most sensitive. This transparency characteristic of the devices is highly favorable for window applications because it allows for a large fraction of visible light to be transmitted.

3. CONCLUSION

Using AgNWs as both the bottom and top electrodes, we achieved ITO-free and fully solution-processed ST-PSCs in a normal structure. The introduction of a layer of ZnO nanoparticles played a crucial role as a mechanical foundation allowing the deposition of top AgNWs by doctor blading. Electrically, the applied ZnO layer enables the formation of quis-ohmic contacts bewteen the active layer and AgNWs and thereby ensures efficient charge extraction. The as-fabricated semitransparent solar cells showed a power conversion efficiency of 2.9% with high FFs of ∼60%, which are comparable to evaporated reference cells. Moreover, the semitransparent AgNW-AgNW cell exhibited a high transmittance of 56% at 550 nm, which offers promising applications for windows, transparent roofs and other transparent architectures. We believe the demonstration of the ITO-free and fully solution-processing route will accelerate the commercialization of the OPV technology, making it a realistic prospect for the near future.

4. EXPERIMENTAL SECTION

Materials. Polymer pDPP5T-2 (batch: GKS1−001, M_w = 47000 g mol^{-1}, PDI = 2.2) was obtained from BASF. PEDOT:PSS (Clevios, P VP AI 4083) was purchased from Heraeus. ZnO nanoparticles dispersed in isopropanol (Product N-10) were kindly provided by Nanograde AG. $PC_{60}BM$ (99.5%) was purchased from Solenne BV. AgNW dispersion (ClearOhm ink) was received from Cambrios Technologies Corp.

Solar Cell Fabrication. All the devices were processed using doctor blading on either glass or ITO-coated glass substrates (both are 2.5 cm × 2.5 cm in size) in ambient atmosphere. Prior to device fabrication, all substrates were cleaned by ultrasonication in acetone and isopropanol for 10 min each. For fully solution-processed AgNW-AgNW cells, the as-received AgNW solution was bladed on glass substrate at 45 °C and subsequently baked at 120 °C to obtain an AgNW layer with thickness of ∼120 nm. After drying, the AgNW-coated glass was subjected to laser patterning to obtain six NW bottom electrodes. Here, a laser fluence of 0.08 J/cm^2 and an overlap of 97.5% were applied to ablate the AgNWs on glass.[31] Subsequently, the as-patterned AgNW electrodes were dipped in distilled water for 30 s to wash away the debris caused by laser patterning. On the prepared AgNW electrodes, a hole transport layer consisting PEDOT:PSS (diluted in isopropanol with volume ratio of 1:3) was deposited at 50 °C and annealed at 140 °C to dry the layer. Afterward, a ∼100 nm-thick active layer pDPP5T-2:$PC_{60}BM$ (1:2 wt %, dissolved in a mixed solvent of 90% chloroform and 10% DCB with a total concentration of 24 mg mL^{-1}) was bladed on top of PEDOT:PSS at 45 °C. The as-received ZnO dispersion was successively coated on top of the active layer at 50 °C and baked at 80 °C to obtain a 40 nm-thick layer. To complete the device fabrication, the top AgNW electrode was bladed on top of ZnO using the same coating parameters that were used on the glass substrate. To expose the bottom NW anodes, the top AgNWs were patterned with scotch tape to remove the two edges, as shown in Figure 3.

For the other three reference devices ITO-Ag, AgNW-Ag and ITO-AgNW, all the solution processed layers were deposited using the same parameters as the device AgNW-AgNW. For the opaque devices, the top Ag electrode was thermally evaporated at a pressure of 5 × 10^{-6} Torr. The effective area of the devices was defined by the overlap of the bottom and top electrodes (∼10.4 mm^2).

Characterizations. The J-V curves were recorded using a source measurement unit from BoTest. Illumination was provided by a solar simulator (Oriel Sol 1A, from Newport) with AM1.5G spectra at 100 mW cm^{-2}, which was calibrated by a certified silicon solar cell. The optical properties of the electrodes and semitransparent devices were measured using a UV−vis-NIR spectrometer (Lambda 950, from PerkinElmer). The thicknesses of the films were measured with a profilometer (Tencor Alpha Step D 100). The EQE spectra were recorded with a Varian CARY 500 Scan spectrometer with a tungsten light source. The AFM images of the AgNWs based films were recorded by Veeco Model D3100 (tapping mode). The cross-section of the AgNW-AgNW device was prepared using a focused ion beam (FIB, FEI Helios NanoLab 660) and subsequently imaged with the electron beam of the same instrument. The laser patterning was performed with an LS 7xxP setup built by LS Laser Systems GmbH (München, Germany).[31]

■ ASSOCIATED CONTENT

Supporting Information

SEM images of the as-coated AgNWs films, wetting behaviors of AgNWs coated on active layer with and without a layer of ZnO nanoparticles, energy level diagram of the semitransparent solar cell AgNW-AgNW, optical microscopy images of laser patterned AgNW electrodes before and after dipping in water, dark $J-V$ curves of the investigated four investigated polymer solar cells, transmittance spectra of the bottom and top AgNW electrodes. This material is available free of charge via the Internet at http://pubs.acs.org/.

■ AUTHOR INFORMATION

Corresponding Authors

* E-mail: Fei.Guo@ww.uni-erlangen.de.
*E-mail: Christoph.Brabec@ww.uni-erlangen.de.

Notes

The authors declare no competing financial interest.

■ ACKNOWLEDGMENTS

This work was financially supported by the Cluster of Excellence "Engineering of Advanced Materials" (EAM) at the University of Erlangen-Nuremberg. The authors thank Saeideh Mohammadzadeh and Prof. Marcus Halik of the Organic Materials and Devices (OMD) group for the access of AFM measurement. K.F. acknowledges use of the services and facilities of the Energie Campus Nürnberg and financial support through the "Aufbruch Bayern" initiative of the state of Bavaria. T.P. acknowledges funding via the DFG research training group GRK 1896. T.S. was funded by a German Research Foundation project grant (DFG; Grant No. BR 4031/1-2). F.G. acknowledges the funding from the China Scholarship Council.

■ REFERENCES

(1) Dennler, G.; Scharber, M. C.; Brabec, C. J. Polymer-Fullerene Bulk-Heterojunction Solar Cells. *Adv. Mater.* **2009**, *21*, 1323−1338.

(2) Krebs, F. C. Fabrication and Processing of Polymer Solar Cells: A Review of Printing and Coating Techniques. *Sol. Energy Mater. Sol. Cells* **2009**, *93*, 394−412.

(3) Guo, F.; Ameri, T.; Forberich, K.; Brabec, C. J. Semitransparent Polymer Solar Cells. *Polym. Int.* **2013**, *62*, 1408−1412.

(4) Chen, C. C.; Dou, L.; Zhu, R.; Chung, C. H.; Song, T. B.; Zheng, Y. B.; Hawks, S.; Li, G.; Weiss, P. S.; Yang, Y. Visibly Transparent Polymer Solar Cells Produced by Solution Processing. *ACS Nano* **2012**, *6*, 7185−7190.

(5) Colsmann, A.; Puetz, A.; Bauer, A.; Hanisch, J.; Ahlswede, E.; Lemmer, U. Efficient Semi-Transparent Organic Solar Cells with Good Transparency Color Perception and Rendering Properties. *Adv. Energy Mater.* **2011**, *1*, 599−603.

(6) Beiley, Z. M.; Christoforo, M. G.; Gratia, P.; Bowring, A. R.; Eberspacher, P.; Margulis, G. Y.; Cabanetos, C.; Beaujuge, P. M.; Salleo, A.; McGehee, M. D. Semi-Transparent Polymer Solar Cells with Excellent Sub-Bandgap Transmission for Third Generation Photovoltaics. *Adv. Mater.* **2013**, DOI: 10.1002/adma.201301985.

(7) Tang, Z.; George, Z.; Ma, Z.; Bergqvist, J.; Tvingstedt, K.; Vandewal, K.; Wang, E.; Andersson, L. M.; Andersson, M. R.; Zhang, F.; Inganäs, O. Semi-transparent Tandem Organic Solar Cells with 90% Internal Quantum Efficiency. *Adv. Energy Mater.* **2012**, *2*, 1467−1476.

(8) Chen, C. C.; Dou, L.; Gao, J.; Chang, W. H.; Li, G.; Yang, Y. High-performance Semi-transparent Polymer Solar Cells Possessing Tandem Structures. *Energy Environ. Sci.* **2013**, *6*, 2714−2720.

(9) Chang, C. Y.; Zuo, L.; Yip, H. L.; Li, C. Z.; Li, Y.; Hsu, C. S.; Cheng, Y. J.; Chen, H.; Jen, A. K. Y. Highly Efficient Polymer Tandem Cells and Semitransparent Cells for Solar Energy. *Adv. Energy Mater.* **2013**, DOI: 10.1002/aenm.201301645.

(10) Yu, W.; Shen, L.; Shen, P.; Menga, F.; Long, Y.; Wang, Y.; Lv, T.; Ruan, S.; Chen, G. Simultaneous Improvement in Efficiency and Transmittance of Low Bandgap Semitransparent Polymer Solar Cells with One-dimensional Photonic Crystals. *Sol. Energy Mater. Sol. Cells* **2013**, *117*, 189−202.

(11) Betancur, R.; Romero-Gomez, P.; Martinez-Otero, A.; Elias, X.; Maymó, M.; Martorell, J. Transparent Polymer Solar Cells Employing a Layered Light-trapping Architecture. *Nat. Photonics* **2013**, *7*, 995−1000.

(12) Yu, W.; Shen, L.; Shen, P.; Long, Y.; Sun, H.; Chen, W.; Ruan, S. Semitransparent Polymer Solar Cells with 5% Power Conversion Efficiency using Photonic Crystal Reflector. *ACS Appl. Mater. Interfaces* **2014**, *6*, 599−605.

(13) Schmidt, H.; Flügge, H.; Winkler, T.; Bülow, T.; Riedl, T.; Kowalsky, W. Efficient Semitransparent Inverted Organic Solar Cells with Indium Tin Oxide Top Electrode. *Appl. Phys. Lett.* **2009**, *94*, 243302.

(14) Ameri, T.; Dennler, G.; Waldauf, C.; Azimi, H.; Seemann, A.; Forberich, K.; Hauch, J.; Scharber, M.; Hingerl, K.; Brabec, C. J. Fabrication, Optical Modeling, and Color Characterization of Semitransparent Bulk-heterojunction Organic Solar Cells in an Inverted Structure. *Adv. Funct. Mater.* **2010**, *20*, 1592−1598.

(15) Krantz, J.; Stubhan, T.; Richter, M.; Spallek, S.; Litzov, I.; Matt, G. J.; Spiecker, E.; Brabec, C. J. Spray-coated Silver Nanowires as Top Electrode Layer in Semitransparent P3HT: PCBM-based Organic Solar Cell Devices. *Adv. Funct. Mater.* **2013**, *23*, 1711−1717.

(16) Colsmann, A.; Reinhard, M.; Kwon, T. H.; Kayser, C.; Nickel, F.; Czolk, J.; Lemmer, U.; Clark, N.; Jasieniak, J.; Holmes, A. B.; Jones, D. Inverted Semi-transparent Organic Solar Cells with Spray Coated, Surfactant Free Polymer Top-electrodes. *Sol. Energy Mater. Sol. Cells* **2012**, *98*, 118−123.

(17) Chen, K. S.; Salinas, J. F.; Yip, H. L.; Huo, L.; Hou, J.; Jen, A. K. Y. Semi-transparent Polymer Solar Cells with 6% PCE, 25% Average Visible Transmittance and a Color Rendering Index Close to 100 for Power Generating Window Applications. *Energy Environ. Sci.* **2012**, *5*, 9551−9557.

(18) Shimada, C.; Shiratori, S. Viscous Conductive Glue Layer in Semitransparent Polymer-Based Solar Cells Fabricated by a Lamination Process. *ACS Appl. Mater. Interfaces* **2013**, *5*, 11087−11092.

(19) Hecht, D. S.; Hu, L.; Irvin, G. Emerging Transparent Electrodes Based on Thin Films of Carbon Nanotubes, Graphene, and Metallic Nanostructures. *Adv. Mater.* **2011**, *23*, 1482−1513.

(20) Angmo, D.; Krebs, F. C. Flexible ITO-free Polymer Solar Cells. *J. Appl. Polym. Sci.* **2012**, *129*, 1−14.

(21) Krantz, J.; Richter, M.; Spallek, S.; Spiecker, E.; Brabec, C. J. Solution-processed Metallic Nanowire Electrodes as Indium Tin Oxide Replacement for Thin-film Solar Cells. *Adv. Funct. Mater.* **2011**, *21*, 4784−4787.

(22) Leem, D. S.; Edwards, A.; Faist, M.; Nelson, J.; Bradley, D. D.; de Mello, J. C. Efficient Organic Solar Cells with Solution-Processed Silver Nanowire Electrodes. *Adv. Mater.* **2011**, *23*, 4371−4375.

(23) Stubhan, T.; Krantz, J.; Li, N.; Guo, F.; Litzov, I.; Steidl, M.; Richter, M.; Matt, G. J.; Brabec, C. J. High Fill Factor Polymer Solar Cells Comprising a Transparent, Low Temperature Solution Processed Doped Metal Oxide/metal Nanowire Composite Electrode. *Sol. Energy Mater. Sol. Cells* **2012**, *107*, 248−251.

(24) Lim, J. W.; Cho, D. Y.; Na, S. I.; Kim, H. K. Simple Brush-painting of Flexible and Transparent Ag Nanowire Network Electrodes as an Alternative ITO Anode for Cost-efficient Flexible Organic Solar Cells. *Sol. Energy Mater. Sol. Cells* **2012**, *107*, 348−354.

(25) Girotto, C.; Rand, B. P.; Steudel, S.; Genoe, J.; Heremans, P. Nanoparticle-based, Spray-coated Silver Top Contacts for Efficient Polymer Solar Cells. *Org. Electron.* **2009**, *10*, 735−740.

(26) Margulis, G. Y.; Christoforo, M. G.; Lam, D.; Beiley, Z. M.; Bowring, A. R.; Bailie, C. D.; Salleo, A.; McGehee, M. D. Spray Deposition of Silver Nanowire Electrodes for Semitransparent Solid-

state Dye-sensitized Solar Cells. *Adv. Energy Mater.* **2013**, DOI: 10.1002/aenm.201300660.
(27) Guo, F.; Zhu, X.; Forberich, K.; Krantz, J.; Stubhan, T.; Salinas, M.; Halik, M.; Spallek, S.; Butz, B.; Spiecker, E.; Ameri, T.; Li, N.; Kubis, P.; Guldi, D. M.; Matt, G. J.; Brabec, C. J. ITO-Free and Fully Solution-Processed Semitransparent Organic Solar Cells with High Fill Factors. *Adv. Energy Mater.* **2013**, *3*, 1062−1067.
(28) Yim, J. H.; Joe, S. Y.; Pang, C.; Lee, K. M.; Jeong, H.; Park, J. Y.; Ahn, Y. H.; de Mello, J. C.; Lee, S. Fully Solution-Processed Semitransparent Organic Solar Cells with a Silver Nanowire Cathode and a Conducting Polymer Anode. *ACS Nano* **2014**, *8*, 2857−2863.
(29) Li, N.; Baran, D.; Forberich, K.; Turbiez, M.; Ameri, T.; Krebs, F. C.; Brabec, C. J. An Efficient Solution-processed Intermediate Layer for Facilitating Fabrication of Organic Multi-junction Solar Cells. *Adv. Energy Mater.* **2013**, DOI: 10.1002/aenm.201300372.
(30) Yu, Z.; Li, L.; Zhang, Q.; Hu, W.; Pei, Q. Silver Nanowire-Polymer Composite Electrodes for Efficient Polymer Solar Cells. *Adv. Mater.* **2011**, *23*, 4453−4457.
(31) Kubis, P.; Li, N.; Stubhan, T.; Machui, F.; Matt, G. J.; Voigt, M. M.; Brabec, C. J. Patterning of Organic Photovoltaic Modules by Ultrafast Laser. *Prog. Photovoltaics Res. Appl.* **2013**, DOI: 10.1002/pip.2421.
(32) Hau, S. K.; Yip, H. L.; Zou, J.; Jen, A. K. Y. Indium Tin Oxide-free Semi-transparent Inverted Polymer Solar Cells using Conducting Polymer as Both Bottom and Top electrodes. *Org. Electron.* **2009**, *10*, 1401−1407.
(33) Girotto, C.; Rand, B. P.; Steudel, S.; Genoe, J.; Heremans, P. Nanoparticle-based, Spray-coated Silver Top Contacts for Efficient Polymer Solar Cells. *Org. Electron.* **2009**, *10*, 735−740.